Techno-Economic Optimization of a Stand-alone PV/PHS/Battery Systems for very low load Situation

Alok Kumar *, Agnimitra Biswas **‡

* Department of Mechanical Engineering, NIT Silchar, Silchar, India, Pin Code: 788 010

** Department of Mechanical Engineering, Assistant Professor, NIT Silchar, Silchar, India, Pin Code: 788 010

(alokkumar.osme@gmail.com, agnibis@yahoo.co.in)

‡ Corresponding Author; Second Author, NIT Silchar, Silchar, India, Pin Code: 788 010, Tel: +91 3842 224879,

Fax: +91 3842 224797, agnibis@yahoo.co.in

Received: 29.07.2016 Accepted:04.05.2017

Abstract- There is hardly any literature on the optimal sizing of solar PV based renewable energy system (RES) with different storage units by using heuristic and meta-heuristic optimization algorithms simultaneously. The objective of this paper is to study the feasibility of pumped hydro storage (PHS) and battery bank storage type solar PV based RES for a very low load (maximum demand less than 30 kW), only to optimise and make the whole system cost effective and storage practically realizable. The modelling for components sizing of the RES is first discussed. Then the individual RESs are techno-economically optimized taking levelized cost of energy (COE) as the objective function at 100% reliability, i.e. 0% unmeet energy (UE) condition. In this, one heuristic optimization algorithm: genetic algorithm (GA), and two meta-heuristic optimization algorithms: Firefly Algorithm (FA) and Grey Wolf Optimization (GWO) are implemented for optimal sizing of the solar PV and the storage systems. Further, their performances are compared by applying these algorithms to an institutional academic block in India. It is shown that GWO is the best optimization algorithm in terms of convergence rate as well as the COE and reliability. The results also demonstrate that utilizing a small battery bank with PHS greatly reduces the upper reservoir capacity, with least excess energy generation. Moreover, the optimal solution has also improved the low load factor of the academic block. Thus the present research contributes as a useful reference to the sizing problem of single resource solar PV based RES with different storage units for very low load situation with the help of different optimization algorithms.

Keywords PV renewable energy system, levelized cost of energy, 100% reliability, low load demand, pumped hydro storage, battery storage, optimization algorithms.

1. Introduction

Solar energy is making a perceptible impact in the life of rural and semi-urban clusters [1-2]. Due to this, hybrid renewable energy system with feasible storage units is considered as stand-alone micro grid for satisfying electrical needs of people residing in isolated areas with no grid facilities. Although such hybrid systems have been commercialized, single resource solar PV based renewable energy systems (RES) with practically feasible energy storage units have not been studied at large, which is important for places where wind is not strong, like the north-eastern part of India. Due to intermittency, unpredictability and stochastic nature of solar energy, feasible as well as scalable energy storage units for uninterrupted power supply is a need of the hour. Scientists and engineers have developed advance energy storage systems with improved efficiency and cost [3-21]. Out of these energy storage technologies, two most popular energy storages successfully applied for renewable energy integration are battery and pumped hydro storage (PHS). Although batteries are not environmental friendly, have short lifecycle, still these are widely used in integration of renewable energy due to their simplicity and high load stability nature [17-21]. PHS, on the other hand, is a suitable and matured solution for large and long-time energy storage as compared to other storage technologies. Some of the real projects in remote villages in which PHS has been successfully used are discussed in

literature [22-25]. In some recent studies, it is seen that small-scale PHS can be successfully integrated into the RES for small island power supply [26-29]. Ma et al. [26-27] reported that PHS based hybrid system is an ideal solution to achieve 100% energy autonomy in remote communities. In [30], it is reported that PHS can successfully be used in stand-alone micro grids if the renewable energy requirement is below 300 kW like that of an island. In some very recent studies, Ma et al. have again performed techno-economic analysis of hybrid RES [28] as well as only solar PV based RES [29] involving PHS for power supply in the scale of few hundred kW.

However, none of these studies have explored the practical feasibility as well as scalability of PHS in integration with single resource solar PV based RES for power supply less than hundred kW. Further for small-scale generation, PHS alone might not be always feasible as well as scalable for small autonomy days and low load demand situation. And even in such a case integration of small scale storage like battery bank can also reduce the load on the PHS and make whole system feasible. For e.g. in [29], the size of the upper reservoir of the optimum design is quite large with 13,205 m3 storage volume and 60 m height. This design in [29] could have been made more feasible by integrating battery bank into the system as well as optimizing the system by using different optimization algorithms simultaneously, which was never done before.

The objective of this paper is to study the feasibility of pumped hydro storage (PHS) and battery bank storage type solar PV based RES for a very low load (maximum demand less than 30 kW), only to optimise and make the whole system cost effective and storage practically realizable. The modelling for components sizing of the RES is first discussed, then the RES is techno-economically optimized taking levelized cost of energy (COE) as the objective function at 100% reliability, i.e. 0% unmeet energy (UE) condition. For this, heuristic GA optimization algorithm and two meta-heuristic optimization algorithms, namely Firefly Algorithm (FA) and Grey Wolf Optimization (GWO) are implemented for optimal sizing of the PV and the storage units to the considered load condition. The methodologies are applied to an institutional academic block in India, only to make the whole system cost effective and storage practically realizable for that load condition. In the subsequent part of the paper, section 2 incorporates the description of the proposed RES model, section 3 incorporates the description of the modeling and sizing of the RES system, section 4 incorporates the description of the energy balance models, section 5 incorporates the cost analysis, which are then followed by description of the optimization algorithms in section 6, results and discussions in section 7, and finally the work is concluded in section 8.

2. Physical model of the RES

The RES is shown in fig.1, which consists of a PV array, pump, turbo-generator, DC-AC converter, upper reservoir (UR), lower reservoir (LR), end-user (load), and battery bank. Here PV power generation first satisfies the load demand then surplus energy goes to pump for elevating the water from a lower reservoir to an upper reservoir and thus energy is stored in the form of gravitational potential energy. In this system two separate penstocks are used, one is for pump and the other for turbine. Hence charging and discharging processes can occur simultaneously. The double penstock system was used in many real projects and by many researchers [31-32]. A small head of 30 meter is considered, and the head is considered fixed in this paper for entire life cycle of the project. Therefore for proper utilization of the surplus energy from the PV array, a number of parallel pumps are used to increase the net flow rate of water. At the time of requirement, water can be drawn-out from the UR and passed through the turbine. By using small battery bank with PHS, the size of UR can be reduced. The battery generally takes the peak hour load and its response to load is very quick as compared to PHS. Hence the power supply to end-user can be very smooth. This type of system has been used in many real projects in the world [29, 33].

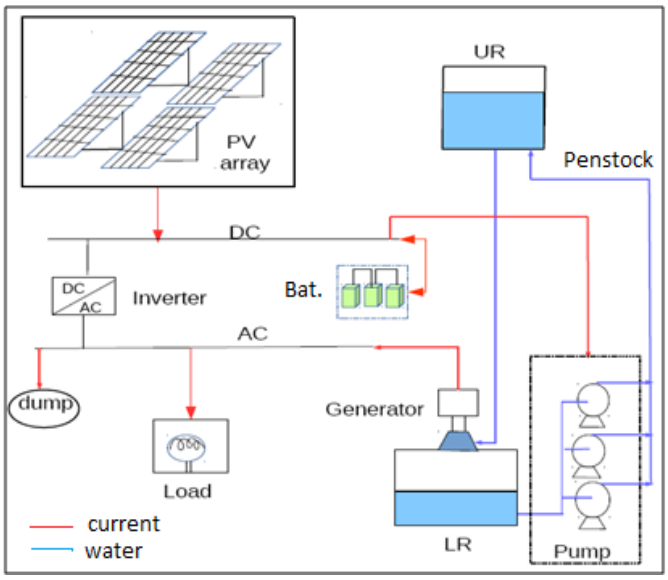

Fig. 1. The block diagram of a stand-alone RES for combined PV, PHS and Battery

3. Modeling and sizing of the RES system

The mathematical equations for individual components of the renewable energy system are proposed in this section. An hour by hour simulation program is then developed to size the PV panel, Battery banks, UR, inverter, pump and turbine.

3.1. PV array modeling

PV panel is a device that directly converts solar radiation into electricity by the virtue of Photoelectric effect. The power output from PV panel is a function of solar insolation and temperature, Eq. (1).

$$P_{PV}(t) = N_{PV} \times Y_{PV} \times \left(\frac{G(t)}{G_o}\right) \times \left[1 + \sigma(T_C - T_O\right] \qquad (1)$$

Neglecting the temperature effect, the above equation becomes-

$$P_{PV}(t) = N_{PV} \times Y_{PV} \times \left(\frac{G(t)}{G_o}\right) \quad (2)$$

Therefore the energy produced in whole day is given in Eq. (3)

$$E_{PV} = \int_0^{24} P_{PV}(t)dt \quad (3)$$

Where $P_{PV}(t)$ is the net power output from PV panel (kW), N_{PV} is the rated capacity of PV panel (kW), Y_{PV} is the PV derating factor, accounting for the factors like aging, soiling, wiring losses, shading, and so on; $G(t)$ is global solar insolation at any time 't'(kW/m^2); G_o is standard global insolation and σ is the Temperature coefficient for power $(1/^oK)$.

3.2. Battery Modeling

The capacity of battery storage in ampere hour) is determined by Eq. (4)

$$C_{Ah} = \frac{(1-\theta)\cdot n_{day}\cdot E_{Load}}{\eta_{b\_eff}\cdot DOD\cdot V_{Bat}} \quad (4)$$

where n_{day} is number of autonomous days, powered absolutely by the battery storage, E_{Load} is the daily energy consumption, V_{Bat} is rated battery voltage, *DOD* is allowable depth of discharge, η_{b_eff} is overall efficiency of battery, and is the portion of power that comes from PV to the load. Charging and discharging current of battery is defined in Eqns. 5 & 6.

$$C_i(t) = \frac{\left(P_{PV}(t) - Load(t)/\eta_{eff}\right)\eta_{b\_eff}}{V_{Bat}} \times 1000 \quad (5)$$

$$D_i(t) = \frac{Load(t)/\eta_{eff} - P_{PV}(t)}{V_{Bat}} \times 1000 \quad (6)$$

Therefore the net charge in battery at any time is determined from Eq. (7)

$$C_{Ah}(t) = C_{Ah}(t-1)(1-\gamma) + \int_{t-1}^{t} C_i(t)dt - \int_{t-1}^{t} D_i(t)dt \quad (7)$$

Where η_{eff} is efficiency of inverter, η_{b_eff} is efficiency of battery, γ is coefficient of self-discharge, C_{Ah} is capacity of battery in Ah and V_{Bat} is nominal voltage of battery.

3.3. Pump modeling

The water flow rate to the upper reservoir from the lower reservoir by the pump is expressed in Eq. (8). The power is directly supplied by the PV panel.

$$q_p(t) = \frac{\eta_p \cdot P_{Pump}(t)}{\rho \cdot g \cdot h} = C_P \cdot P_{Pump}(t) \quad (8)$$

Where P_{Pump} is power from the PV panel supplied to the pump (kW), h is the total head (m), g is the acceleration due to gravity (9.8 m/s^2), ρ is water density (1000 kg/m^3), η_p is the overall pumping efficiency, and C_p is the water pumping coefficient of the pump (m^3/kWh). Therefore, total amount of water pumped in an hour is given by Eq. (9)

$$Q_P(t) = \int_0^t q_P(t)\cdot dt \quad (9)$$

The total number of pumps needed is decided by:

$$N_{Pump} = \frac{P_{\max}}{P_o} \quad (10)$$

Where $P_{\max}$ is maximum amount of surplus power from PV array (kW), P_o is rated power of single pump (kW).

3.4. Turbine Modeling

In the case of energy deficiency, water is drawn from the upper reservoir in order to operate the turbines. The released power from the turbine at any given time is:

$$P_T(t) = \eta_T \cdot \rho \cdot g \cdot h \cdot q_T(t) = C_T.q_T(t) \quad (11)$$

Where η_T is the overall efficiency (including pipe efficiency) of the turbine, $q_T(t)$ is the volumetric flow rate of water towards the turbine (m^3/s), C_T is the coefficient of turbine (kWh/m^3). Therefore, total amount of water input into the turbine in an hour is given by Eq. (12)

$$Q_T(t) = \int_0^t q_T(t)\cdot dt \quad (12)$$

3.5 Upper reservoir (UR) Modeling

The water quantity stored in the UR should be sufficient to satisfy power demand in case of no power supply for several consecutive days [26, 29]. The water level in the UR can be considered as the state of charge (SOC) of the storage tank. The gravitational-potential energy stored in the UR is given by-

$$E_{Cap} = \theta \cdot n_{day} \cdot E_{load} = \frac{\eta_T \cdot \rho \cdot V_{UR} \cdot g \cdot h}{3.6\times 10^6} \quad (13)$$

Where E_{Cap} is the energy storage capacity of a water reservoir (kWh); V_{UR} is the volume or storage capacity of the water reservoir (m^3). Therefore, the total quantity of water stored in the UR at any time 't' is determined by:

$$Q_{UR}(t) = Q_{UR}(t-1)(1-\alpha) + Q_P(t) - Q_T(t) \quad (14)$$

Where α (0.05) is the evaporation and leakage loss. The water quantity of the upper reservoir will be subject to the following constraints:

$$Q_{UR\min} \le Q_{UR} \le Q_{UR\max} = V_{UR} \quad (15)$$

$$SOC(\%) = \frac{Q_{UR}(t)}{V_{UR}} \times 100 \quad (16)$$

$Q_{UR\min}$ is the maximum water stored in UR, which is usually set as zero.

4. Energy Balance Models for Power Generation and load Consumption

The generalized energy balance model of the solar power generation system at time t is expressed as:

$$P_{PV}(t) \cdot \eta_{inv.} = P_L(t) + P_{Pump}(t) + P_{Bat.}(t) + P_{Dump}(t) \quad (17)$$

Where $\eta_{inv.}$ is the inverter efficiency, which is the ratio of the inverter's AC output power to DC input power, $P_L(t)$ is the solar power output directly delivered to the load; $P_{Pump}(t)$ is the power transferred to the pumps for charging Upper reservoir; $P_{Bat.}(t)$ is the power transferred to the battery and $P_{Dump}(t)$ is the excess energy delivered to a dump load. The load demand is mainly covered by three sources, so the energy balance mode of load consumption is given by

$$P_{TL}(t) = P_L(t) + P_{Turbine}(t) + P_{Bat.}(t) \quad (18)$$

Where $P_L(t)$ is the power directly delivered from the RES generator; $P_{Turbine}(t)$ is the power produced by the turbo-generator, $P_{Bat.}$ is the power produced by the battery. When the net load is negative or zero, no supplementary energy is required and thus $P_{Turbine}(t)$ and $P_{Bat.}$ are zero

5. Cost Analysis

In this study, total life cycle cost (LCC) is used to analyze the system's economic performance. LCC includes the cost of construction (CC) including the installation cost of the single resource solar PV system, replacement cost (RC), and operating and maintenance (O&M) cost. Replacement cost is considered as the depreciation cost, which is considered 10% of the cost of construction. The total life cycle cost (LCC) can be calculated according to Eq. (19)

$$LCC = CC + O\&M + RC \quad (19)$$

a) Interest rate

The annual interest rate is the discount rate used to convert one-time costs into annualized costs. It is related to the nominal interest rate [33].

$$i = \frac{i' - f}{1 + f} \quad (20)$$

Where i is the interest rate, i' nominal interest rate, and f is the annual inflation rate.

b) Replacement cost

The total replacement cost (RC) of main components is given by-

$$RC = \sum_{i}^{N} [C_{rep_i} \times f_{rep_i} \times SFF_i - S_i \times SFF] \quad (21)$$

Where f_{rep_i} is a factor arising because the component lifetime can be different from the project lifetime, which is defined in Eq. (22)

$$f_{rep_i} = \frac{CRF}{CRF_i} \quad (22)$$

SFF = Sinking Fund Factors is defined as in Eq. (23)

$$SFF = \frac{i}{(1+i)^{n-1}} \quad (23)$$

Then selvage value of the components is define as in Eq. (24)

$$S = C_{rep} \times \frac{L_{rem}}{L_{comp}} \quad (24)$$

Where L_{rem} is remaining life of components, L_{comp} is total life of components, and C_{rep} is the replacement cost factor. CRF is Capital recovery factor, which is defined as in Eq. (25)

$$CRF = \frac{i(1+i)^n}{(1+i)^n - 1} \quad (25)$$

So, the total Annualized Life Cycle Cost (ALCC) is defined as in Eq. (26)

$$ALCC = LCC \times CRF \quad (26)$$

Where 'n' is life of project.

c) Cost information of the components

The cost of major components, namely PV module, Battery, Pump, Turbine, Inverter and Reservoir are taken as per market rate. The capital cost, O & M cost and replacement cost of all the components have been considered. A summary

of the cost information about the major components and their corresponding lifespan is presented in Table 1. The project life is assumed as 25 years.

Table 1. Major components cost and life

Component	**Unit Capital Cost($)**	**Life cycle (Year)**	**Replacement cost ($)**	**O & M cost $/kW-year % of capital cost**
PV panel (200kWp)	300	25	200	0.2%
Battery	65	3	65	00%
Inverter	900/kW	15	900	0.5%
Solar DC pump	230 /kW	10	180	0.5%
Turbine with pipes	600/kW	10	400	0.5%
Upper reservoir	150/m^3	35	150	0.5%

Table 2. Some constant parameter

Parameter	**Value**
Battery efficiency (η_{b_eff})	85%
Inverter efficiency (η_{inv})	92%
Pumping efficiency (η_p)	80%
Turbine efficiency (η_T)	70%
Derating factor (Y_{PV})	85%
Total head (h)	30 m
Nominal interest ($i^{'}$)	7%
Annual interest due to inflation(f)	4%
Life of project (n)	25 years

d) Levelized cost of energy (COE)

The levelized cost of energy (COE) is considered as a principal cost of economics for figuring out the merit of the all the systems. It is a ratio of the annualized life cycle cost of the system to the daily energy demand. In other word it is the cost per unit electricity generated ($/kWh).

$$COE = \frac{ALCC}{E_{Load}} \tag{27}$$

The nominal interest rate and annual inflation rate along with other parameters are provided in Table 2. In table 2, derating factor of 85% is considered. In electronics, derating is the operation of a device at less than its rated maximum capability in order to prolong its life. Therefore, derating factor of 85% implies that solar PV system is assumed to be operated at 85% of its rated capacity.

6. Optimization Algorithms through Heuristic and Meta-Heuristic approaches

In this work, for finding out the least possible value of COE for each system, three well-known optimization algorithms, namely Genetic algorithm (GA), firefly algorithm (FA), and Grey wolf optimization (GWO) have been applied simultaneously.

6.1 Heuristic Approach

Genetic algorithms are categorized as global search heuristics approaches. Basically the GA optimization is inspired by natural evolution, such as inheritance, mutation, selection, and cross over which is well demonstrated in fig.2 [34-35]. In GA the evolution usually starts from a population of randomly generated individuals and that continues in generations. In each generation, the fitness of every individual in the population is evaluated, then multiple individuals are selected from the current population (based on their fitness function), and they are modified (recombined and possibly mutated) to form new population/generation. The new generation is then used in the next iteration of the algorithm. Commonly, the algorithm terminates when either

a maximum number of generations has been performed, or a satisfactory fitness level has been reached for the population.

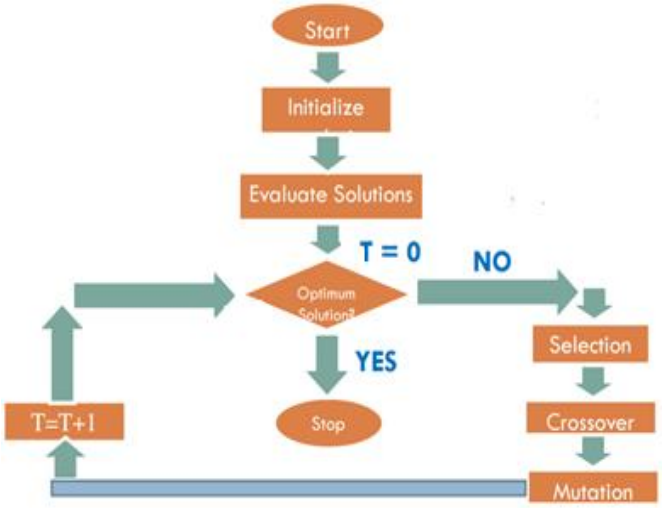

Fig. 2. Flow chart of GA Optimization

6.2 Meta-Heuristic Approach

Meta-heuristic optimization approaches have wieldy used and these have become very popular over the last two decades because of their simplicity, flexibility, derivation-free mechanism, and local optima avoidance.

6.2.1 Firefly algorithm

Firefly algorithm (FA) is a meta-heuristic and natural-inspired algorithm, developed by Yang in late 2007-2008 [36]. Three flashing idealizing characteristics of fireflies to develop firefly inspired algorithm are:-

- Fireflies are having same gender such that one firefly will be attracted to other fireflies regardless of their gender.
- Its attractiveness is proportional to the brightness, and they both decrease as their distance increases.
- The firefly's brightness is determined by the landscape of the objective function.

6.2.1.1 Mathematical Modeling and Algorithm for FA

The attractiveness of fireflies is directly proportional to intensity of light, i.e. the variation of attractiveness of 'β' with distance of 'r', which is given by Eq. (28)

$$\beta = \beta_o e^{-\gamma r^2} \tag{28}$$

Where is absorption coefficient and

$$\beta = \beta_o \text{ at } r = 0 \tag{29}$$

In order to attract next brighter firefly 'j' by the previous firefly 'i', the vector traced at time (t+1) is determined by Eq. (30)-

$$X_i^{t+1} = X_i^t + \beta_O e^{-\gamma r_{i,j}^2}(X_j^t - X_i^t) + \alpha_t \varepsilon_i^t \tag{30}$$

First term is the random vector number at time't', the second term is for attraction, and the third term is for the randomization with having α_t as randomizer. ε_i^t is Gaussian distribution of random vector number at time't'.

The α_t is taken for parameter controlling during the iterations which is defined as Eq. (31)

$$\alpha_t = \alpha_O \delta^t, (0 < \delta < 1) \tag{31}$$

But in most of the cases the value of δ lies between 0.95 and 0.97, and α_0 = 0.1L where L is average scale of the problem. The initial guess value of variables is taken as per Eq. (32)

$$U_0 = Lb + (Ub - Lb) \times rand(size(Lb)) \tag{32}$$

Where U_0 is initial value of the variable; Lb and Ub is lower and upper bound values of the given variable. Figure 3 summarizes the algorithm for the FA.

6.2.2 Grey Wolf Optimization

The Grey Wolf Optimization (GWO) is a latest and most popular meta-heuristic algorithm developed by Mirjalili et al. [37] in 2014, which is inspired from the grey wolves in nature. The wolves have been categorized in four types such as alpha (α) - "The leaders of the group"; beta (β) - "The subordinate wolves that help the leaders"; delta (δ) - "The third level wolves who submit to α and β" and omega (ω) - "The lowest ranker wolves of group who have surrendered to all the other governing wolves". And these four are employed for simulating the leadership hierarchy. This algorithm uses three main steps of hunting; at first searching for prey (exploration), then encircling prey, and finally attacking prey (exploitation). The GWO algorithm is benchmarked on 29 most popular test functions, and the GWO has been able to provide highly competitive results compared to very popular heuristics and Meta-heuristic approaches. The GWO algorithm has showed its high performance in the unconstrained as well as in constrained type problems [38-40]. The convergence process of GWO is quite fast as compared to other algorithms.

6.2.2.1 Mathematical Modeling and Algorithm for GWO

The encircling modeling behaviour of wolves at current iteration 't', at $\vec{X}_P$ position vector of prey and with $\vec{X}$ position vector of wolf is written as Eq. (33-36) [37].

$$\vec{D} = \left| \vec{C} \cdot \vec{X}_P(t) - \vec{X}(t) \right| \quad (33)$$

$$\vec{X}(t+1) = \vec{X}_P - \vec{A} \cdot \vec{D} \quad (34)$$

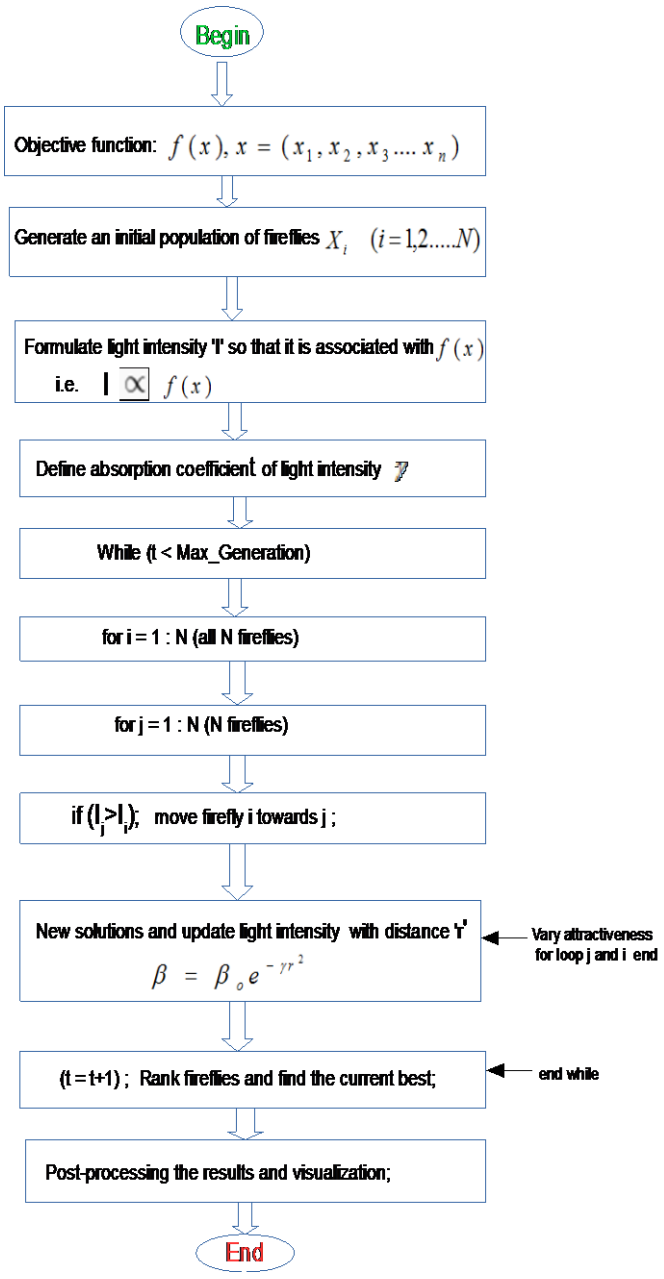

Fig. 3. FA algorithm flow chart

$$\vec{A} = 2\vec{a} \cdot \vec{r}_1 - \vec{a} \quad (35)$$

$$\vec{C} = 2\vec{r}_2 \quad (36)$$

$\vec{A}$ and $\vec{C}$ are coefficients of the position vector, $\vec{a}$ is a linearly deceased vector from 2 to 0 over the maximum iterations and $\vec{r}_1$ and $\vec{r}_2$ are the random vectors in the range of [0,1] as depicted in Eqs. (37-43).

$$D_\alpha = \left| \vec{C}_1 \cdot \vec{X}_\alpha - \vec{X} \right| \quad (37)$$

$$D_\beta = \left| \vec{C}_2 \cdot \vec{X}_\beta - \vec{X} \right| \quad (38)$$

$$D_\delta = \left| \vec{C}_3 \cdot \vec{X}_\delta - \vec{X} \right| \quad (39)$$

$$X_1 = \vec{X}_\alpha - \vec{A}_1 \cdot \vec{D}_\alpha \quad (40)$$

$$X_2 = \vec{X}_\beta - \vec{A}_1 \cdot \vec{D}_\beta \quad (41)$$

$$X_3 = \vec{X}_\delta - \vec{A}_3 \cdot \vec{D}_\delta \quad (42)$$

$$\vec{X}(t+1) = \frac{\vec{X}_1 + \vec{X}_2 + \vec{X}_3}{3} \quad (43)$$

Here alpha 'α' is taken as the best fittest solution of the objective function, beta 'β' and delta 'δ' are second and third best solutions, and rest of all the solutions are taken as omega 'ω'. Fig.4 summarizes the GWO algorithm.

6.3 Optimization Strategy

In the Single-objective optimization, the main objective is to minimise the value of COE. Three optimization techniques such as GA, GWO and FA have been used to find out the least possible value of the levelized cost of energy (COE). The COE is taken as the fitness function without any type of power faliure i.e. 100% reliability of power supply to the load. The optimization algorithm have been run on MATLAB 2014 Software. The fitness function for all three proposed configration is shown in Eq (44).

$$Z\_\min = f(COE) \quad (44)$$

$UE = 0\%$ is taken as the constraint. The lower and upper bounary of NPV,CAh and VUR are given in Eqs. (45-47).

$$100 \le N_{PV} \le 1000 \quad (45)$$

$$50 \le C_{Ah} \le 8000 \quad (46)$$

$$100 \le V_{UR} \le 5000 \quad (47)$$

Where NPV= size of PV panel (kW), Ah= capacity of battery, V_{UR} = upper reservoir volume (m^3). The above objective function has one indirect constraint (UE %). And hence in optimization-tool box of GA, which is inbulit in the MATLAB Software, the following have been considered:

- The constraints box remains empty.
- In the population box "Feasible population" is selected.
- The "Stochastic uniform" is selected in selection function box.
- 0.05*population size default function is chosen for reproduction function box. And cross-over fraction is 0.8 as default value.
- In the Mutation function box "Adaptive feasible" is selected.
- The "Heuristic function" is chosen for cross-over function with having 1.2 default ratio.

- Then the "Forward direction of migration" is used.
- Finally, the number of generations is selected as "200" for all the three systems.

Similary for firefly algorithm (FA) the following parameters have been used

- Number of searching agent (fireflies) / population = 20.
- The maximum number of genetarions/iteration = 300
- Number of variables for the system (i.e. PV/PHS/Bat) is three.
- The lower bound [Lb] and upper bound [Ub] of variable are considered as per Eqs. (45-47).

For the GWO algorithm the following parameters have been used:-

- The number of searching agents wolves)/population = 20.
- The maximum number of iterations/generations
- = 300
- Number of variables for the system (i.e. PV/PHS/Bat) is three.
- Some default constants for alpha (α), beta (β), and gamma (γ) are 0.5, 0.2 and 0.1 respectively.
- The lower bound [lb] and upper bound [ub] of variable are considered as per Eqs. (45-47).

The system optimization process flow chart for the PV/ Bat. /PHS is illustrated in fig.5. The optimization process starts with the random guess value of the system variables (like size of PV modules, size of battery capacity and size of UR) then consequently runs through all the steps of the algorithms, and continues until archives stop category or reaches max-iteration/ max-generations. In this, SOC of battery is taken between 50% and 90%. With this the battery life can be improved because the high depth of discharge and over charge are usually harmful for the battery.

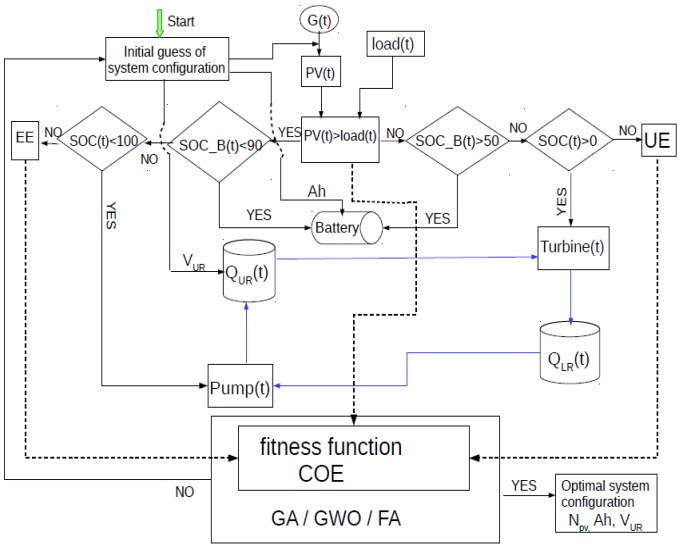

Fig. 5. Flow chart of Optimization PV/ Bat/ PHS

6.4 System Reliability Model

In this study, the system reliability is evaluated based on the percentage of unmeet energy (UE) per year, which is defined as the total power supply failure divided by the total energy demand over a year [26, 40-41]. The reliability study is done to evaluate whether a system is able to fulfill the load demand, and if there is any deficiency, then to calculate the percentage of insufficient energy. Another most important index which is widely used is percentage of excess energy (EE) in a year. The index UE and EE are calculated as follows in Eqs. (48, 49) respectively.

$$UE(\%) = \frac{\sum_{1}^{8760} P_{TL}(t) > [P_L(t) + P_{Turbine}(t)]}{E_{Load}} \times 100 \quad (48)$$

$$EE(\%) = \frac{\sum_{1}^{8760} P_{Dump}(t)}{\sum_{1}^{8760} P_{PV}(t)} \times 100 \quad (49)$$

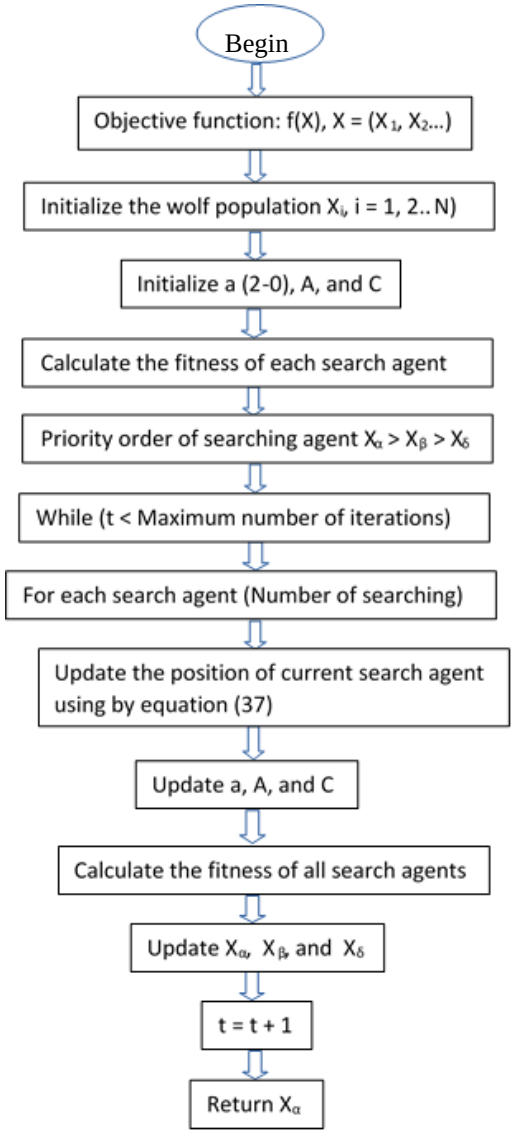

Fig. 4. GWO algorithm flow chart

7. Results and Discussions

The proposed RES system is employed in an institutional academic block with low load factor, which is situated in north-eastern India. This academic block is a 4-storey building, which consists of large rooms for laboratories and faculty cabins. A survey for the electricity consumption of the building was conducted for collecting all these load data. Figures 6 and 7 show the hourly variation of load for winter and summer respectively. As can be calculated, the load factors of both the seasons are very low, which is around 0.131 during both winter and summer. The load factor is defined as the ratio of the average load to the peak load. Also the daily average energy consumed is also quite low, which is 88.7 kWh. The major load requirement during weekdays in any season occurs during the afternoon time due to laboratory classes that are conducted then. The weekend load is lower due to less running of the major equipment and machineries of the academic block.

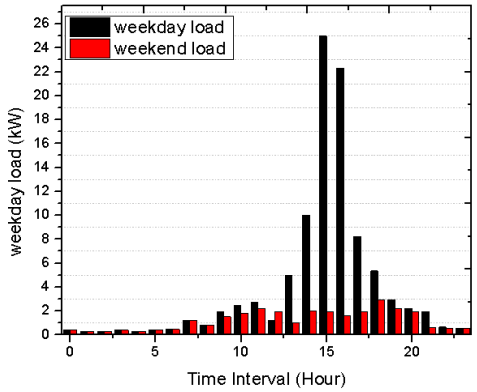

Fig. 6. Daily electricity demand variation for the winter

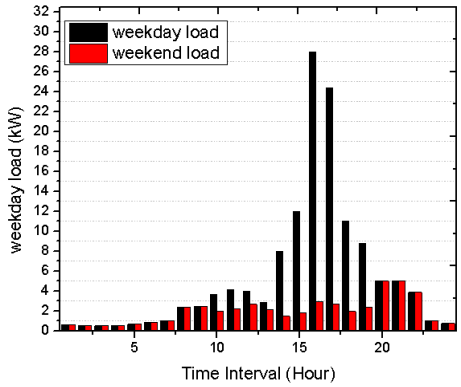

Fig. 7. Daily electricity demand variation for the summer

7.1 For combination of PV and PHS with 0% UE

Figure 8 shows that for GA, the converged COE is \$1.3626/ kWh, which is obtained after 60 generations. Now, it can be observed from fig.9 that both GWO and FA techniques give the same least value of COE, i.e \$ 1.3193/ kWh, having PV array of 180 kW (1258.74 m^2), pump size of 150 kW, turbine size of 28 kW, upper reservoir of size 2244.5 m^3 and inverter size of 32 kW as shown in table 3. Besides PV capacity, values of all other parameters are less than those obtained by GA. In this case, the GWO converges faster than the FA and GA as shown in fig. 9, which happens just after 40 generations.

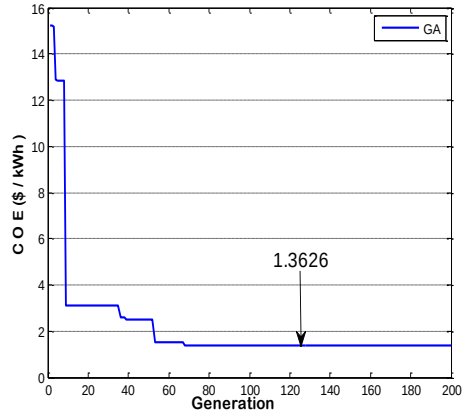

Fig. 8. Converged curve (variations of COE during GA optimization process)

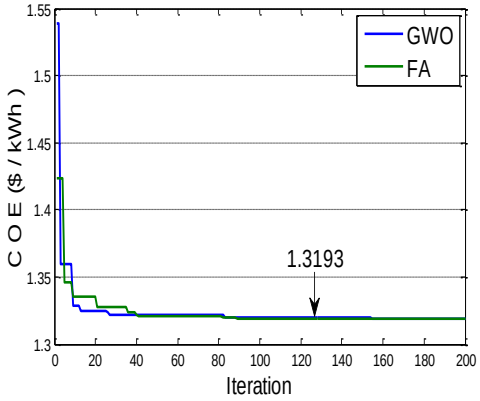

Fig. 9. Converged curve (variations of COE during GWO & FA optimization process)

7.2 For combination of PV, PHS and Battery with 0% UE

By integrating the battery bank in the RES, the simulations are run, and the results are represented in fig.10 & 11. In this case also GWO converges faster than the FA (less than 10 iterations), and GA converges later after 150 generations. FA converges in between that of GA and GWO. The GWO has converged at \$0.9109/kWh whereas FA and GA have converged at \$0.9116/ kWh and \$0.9632/ kWh respectively. Therefore, GWO is the best algorithm in terms of convergence rate as well as the COE. Further, integrating battery banks seems to be more feasible for this low load demand situation as the COE has decreased below than the combinations of only PV and PHS. The optimal sizes of components obtained from GWO are 142.90 kW of PV panel, 1192.50 m^3 of UR, battery banks of 1811.7 Ah, 97.083 kW of pump and 22.164 kW of turbine as shown in table 4. Moreover, using small size battery banks with PHS, the size of UR has greatly reduced (from 2244.5 m^3 down to 1192.50 m^3). And the excess energy has also decreased as compared to the previous combination of only PV and PHS, which is 25.26 kW as compared to 35.07 kW.

Table 3: Results of optimization of the combinations of PV and PHS

PV/PHS	Cost($/kWh)	Excess Energy (%)	PV (kW)	Ur (m^3)
GA	1.3626	39.078	164.94	2554.3
FA	1.3193	35.075	180	2244.5
GWO	1.3193	35.075	180	2244.5

Table 4: Results of optimization of the combinations of PV, PHS, and Battery

PV/Battery/PHS	Cost($/kWh)	Excess Energy (%)	PV (kW)	Bat (Ah)	Ur (m^3)
GA	0.9632	27.828	142.37	1720.672	1229.650
FA	0.9116	25.46	143.15	1722.50	1193.90
GWO	0.9109	25.26	142.90	1811.70	1192.50

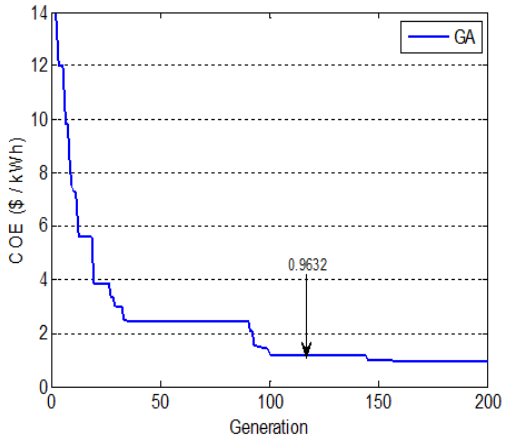

Fig. 10. Converged curve (variations of COE during GA optimization process)

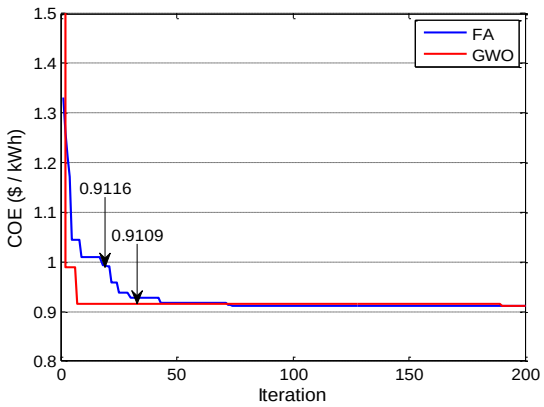

Fig. 11. Converged curve (variations of COE during GWO & FA optimization process)

Three to four trials have been performed for each algorithm. After this the converged value does not change much. As all these algorithms are based on random selection of initial value, therefore usually during the iterations of each trail, the initial value and the convergence curve do not remain the same. However after 80-100 iterations in each trial, the value of COE converges to a fixed value (Fig. 8-11). The average time elapsed for say 200 iterations is 3 to 4 hrs in each trial. Here the speed of iteration depends on the specification of computer. In this case, it is Intel Core i7-2600 3.4GHz Processor.

A plot of hourly load shearing simulation curve for the combinations of PV, Battery, and PHS of a sample day is shown in Fig.12. In this plot it can be seen that battery is charging at first directly from the PV power till noon time. After 90% SOC of the battery, pump start pumping the water from lower reservoir to upper reservoir immediately before the noon time. Due to evaporations, SOC (%) of upper reservoir has decreased during the battery charging hours (5:00 am to 12:00 am). The turbine has started when the SOC of battery goes below 50% at about 4 p.m. after which the turbine meets the load of the building throughout the night as can be seen from fig.12. and for which the SOC of upper reservoir starts decreasing. There is no excess energy generated during that sample day and also no loss of power supply has occurred, except a small dump load generating between 12 o'clock and 5 o'clock due to the combined SOC of the upper reservoir and the battery bank. During the whole year, the net amount of electricity generated through the PV is 191,300 kWh, in which the peak power production is 128.203 kW. The electricity produced by PV panel is divided into four parts. About 80,971 kWh (42.33%) is transferred to the water-pumping units, and 32.41% directly goes to the load and battery banks. However, about 25.26% of the total PV production is dissipated in the form of dump load. The

simulated plot also demonstrates that the academic block's load has been balanced very well with this system. Figure 13 shows the comparison between the new load profile as generated by the optimal solution and the building actual load profile for a single day. It can be noted that at first part (day-time) the energy is stored in batteries in the form of electro-chemical energy and consequently in UR in the form of gravitational potential energy; in second part, this energy is dispatched to cater the load demand (firstly from batteries and afterwards from UR). The load factor of new load profile is 0.308, whereas actual load factor of building is 0.131, and hence load factor is improved by 0.177. The reason for the increase of load factor is due to higher load sharing by the RES before noon than the grid connected building load profile. Figure 14 illustrates the sharing of LCC among its components for the proposed configuration. 82% of LCC of the system is attributed by PV and UR; however rest 18% of LCC is shared by all other components of the system. The net annualized LCC for this optimal configuration is $29,214 and corresponding COE is $0.9109. In this configuration, the higher cost item is PV panels ($225,070) and least cost item is turbine ($15,467).

Figure 15 illustrates the relative frequency of battery's SOC (%) and UR's SOC (%) for the entire year. The battery SOC is within 50% to 90% whereas for UR it is from 0% to 100%. It can be observed that higher percentage of distribution frequency for battery lies within 70% to 80% (i.e. 47.91%) whereas that for UR lies within 80% to 90% (i.e. 45.81%). Here about 47825 kWh of excess electricity is produced during the 8760 hrs time, which is near about 25.26% of total PV power production in a year, which is quite small. The results indicate that the maximum percentage of relative frequency (about 21.14%) of its SOC values lies within 80% to 90%. The relative frequency of 12.59% has occurred for 90% to 100% of SOC. Here it can be noted that the high relative frequency percentage of its SOC lies below 90% for both the storage units, i.e. for UR 45.81% of relative frequency has occurred for 80% to 90% of SOC, and for battery bank 47.81% of relative frequency has occurred for 70% to 80% of SOC.

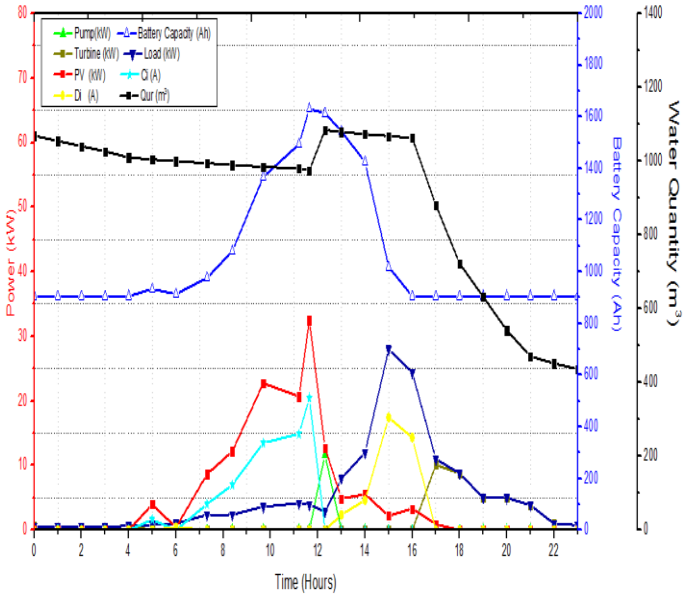

Fig. 12. Hourly energy balance curve on sample day

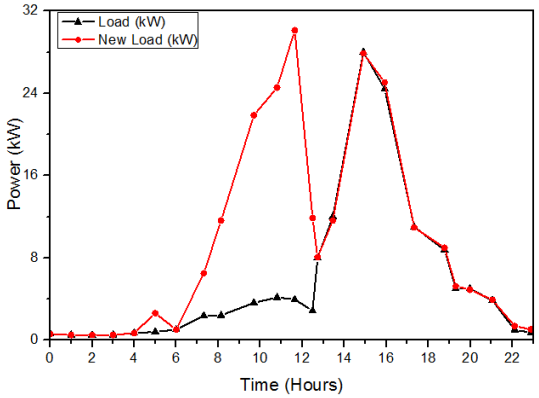

Fig. 13. The new load and actual load profile

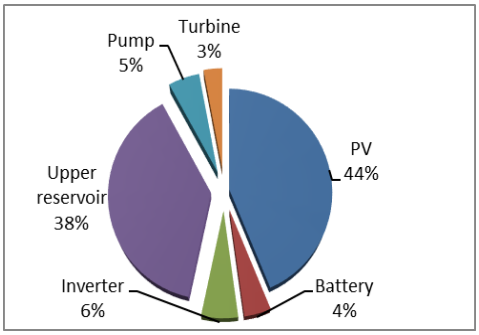

Fig. 14. Break-down of LCC by components

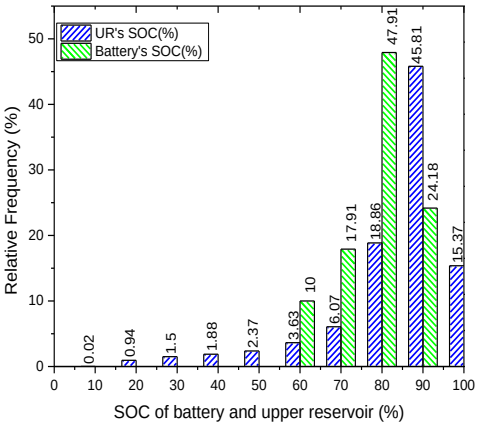

Fig. 15. The relative frequency v/s UR SOC

8. Conclusions

The objective of this paper is to study the feasibility of pumped hydro storage (PHS) and battery bank storage type solar PV based RES for a very low load (maximum demand less than 30 kW), only to optimise and make the whole system cost effective and storage practically realizable. From the study the following conclusions can be summarized:

a) The GWO is found to be the best optimization algorithm in terms of convergence rate as well as the COE and reliability. Combined PV, PHS and battery based RES is found to be the optimal solution for the given low load situation compared with only PV and PHS based RES. The optimal solutions are 142.90 kW of PV panel, 1192.50 m^3 of

UR, 1811.7 Ah of battery banks, 97.083 kW of pump and 22.164 kW of turbine.

b) Utilizing a small battery bank with the PHS greatly reduces the upper reservoir capacity (2244.5 m^3 to 1192.50 m^3), and improves the power supply reliability with least excess energy of 25.26 kW as compared to 35.07 kW for only PV and PHS based RES.

c) For the combined PV, PHS and battery based RES, the high value of relative frequency of the SOC for UR and battery banks has occurred for below 90% of SOC, and due to this the percentage of excess energy (EE) is greatly reduced.

d) The load factor of the new load profile generated by the optimal solutions is 0.308. Hence the optimal solution of combined PV, PHS and battery based RES has improved the low load factor of the academic block.

Thus the present research contributes as a useful reference to the sizing problem of single resource solar PV based RES with different storage units for very low load situation with the help of different optimization algorithms.

References

[1] Das H.S, Dey A, Wei T.C, Yatim A.H.M. Feasibility Analysis of Standalone PV/Wind/Battery Hybrid Energy System for Rural Bangladesh. International Journal of Renewable Energy Research 2016; 6(2): 402-412.
[2] Kolhe M, Kolhe S, Joshi J.C. Economic viability of stand-alone solar photovoltaic system in comparison with diesel-powered system for India, Energy Econ. 2002; 24: 155–165.
[3] Rabiee A, Khorramdel H, Aghaei J. A review of energy storage systems in micro grids with wind turbines. Renew Sustain Energy Rev 2013; 18:316–26.
[4] Rahman F, Rehman S, Abdul-Majeed MA. Overview of energy storage systems for storing electricity from renewable energy sources in Saudi Arabia. Renew Sustain Energy Rev 2012; 16:274–83.
[5] Francisco D, Sumper A, Oriol G, Roberto V. A review of energy storage technologies for wind power applications. Renew Sustain Energy Rev 2012; 16 (4):2154–2171.
[6] Ghiani E, Mocci S, Celli G, Pilo F. Increasing the flexible use of hydro pumping storage for maximizing the exploitation of RES in Sardinia. In: Proceedings of 3rd IEEE conference on Renewable power generation, 24-25 Sept. 2014, pp 1-6.
[7] Kaldellis J, Zafirakis D, Kondili E.M. Optimum sizing of photovoltaic-energy storage systems for autonomous small islands, International Journal of Electrical Power & Energy Systems 2010; 32(1): 24-36.
[8] Succar S, Denkenberger D.C, Williams R.H. Optimization of specific rating for wind turbine arrays coupled to compressed air energy storage. Appl Energy 2012; 96:222–34.
[9] Serban I, Marinescu C. Battery energy storage system for frequency support in micro grids and with enhanced control features for uninterruptible supply of local loads. Int J Electr Power Energy Sys 2014; 54:432–41.
[10] Okou R, Sebitosi A.B, Pillay P. Flywheel rotor manufacture for rural energy storage in sub-Saharan Africa. Energy 2011; 36:6138–45.
[11] Dagdougui H, Minciardi R, Ouammi A, Robba M, Sacile R. Modeling and optimization of a hybrid system for the energy supply of a Green building. Energy Convers Manage 2012; 64:351–363.
[12] Zhao J, Wang C, Zhao B, Lin F, Zhou Q, Wang Y. A review of active management for distribution networks-current status and future development trends. Electr Power Compon Syst 2014; 42:280–293.
[13] Gustavsson M, Mtonga D. Lead-acid battery capacity in solar home systems- field tests and experiences in Lundazi, Zambia, Sol Energy 2005; 79:551–558.
[14] Krieger E.M, Cannarella J, Arnold C.B. A comparison of lead-acid and lithium based battery behaviour and capacity-fade in off-grid renewable charging applications. Energy 2013; 60:492–500.
[15] Hadjipaschalis I, Poullikkas A, Efthimiou V. Overview of current and future energy storage technologies for electric power applications. Renew Sustain Energy Rev 2009; 13 (6-7):1513–1522.
[16] Baker J. New technology and possible advances in energy storage. Energy Policy 2008; 36:4368–4373.
[17] Depernet D, Ba O, Berthon A. Online impedance spectroscopy of lead acid batteries for storage management of a standalone power plant. Power Sources 2012; 219:65–74.
[18] Nair N.C, Garimella N. Battery energy storage systems: assessment for small-scale renewable energy integration. Energy Build 2010; 42 (11):2124–2130.
[19] Mahmoud M.M. On the storage batteries used in solar electric power systems and development of an algorithm for determining their ampere–hour capacity, Electr Power Syst Res 2004; 71:85–89.
[20] Shaahid S.M, AElhadidy M. Technical and economic assessment of grid independent hybrid photovoltaic-diesel-battery power system for commercial load in desert environments, Renewable and Sustainable Energy Review 2007; 11: 1794-1810.
[21] Hoppmann J, Volland J, Schmidt T.S, Hoffmann V.H. The economic viability of battery storage for residential solar photovoltaic systems– A review and a simulation model, Renewable and Sustainable Energy Reviews 2014; 39: 1101–1118.
[22] Anagnostopoulos J.S., Papantonis D.E. Study of pumped storage schemes to support high RES penetration in the electric power system of Greece, Energy 2012; 45 (1): 416-423.
[23] Connolly D, Lund H, Mathiesen B.V, Pican E, Leahy M. The technical and economic implications of integrating fluctuating renewable energy using energy storage, Renew Energy 2012; 43:47–60.
[24] Manolakos D, Papadakis G, Papantonis D, Kyritsis S. A stand-alone photovoltaic power system for remote villages using pumped water energy storage, Energy 2004; 29:57–69.
[25] Compilation and Analysis of information on existing rural electrification and renewable energy programmes

in the province of Oudomxay, Lao PDR (final report). SUNLABOB Rural Energy Systems Ltd., Lao PDR; October 2007.

[26] Ma T, Yang H, Lu L, Peng J. Technical feasibility study on a standalone hybrid solar-wind system with pumped hydro storage for a remote island in Hong Kong. Renewable Energy 2014; 69:7–15.

[27] Ma T, Yang H, Lu L. Feasibility study and economic analysis of pumped hydro storage and battery storage for a renewable energy powered island. Energy Conversion and Management 2014; 79: 387-397.

[28] Ma T, Yang H, Lu L, Peng J. Optimal design of an autonomous solar–wind-pumped storage power supply system. Applied Energy 2015; 160: 728-736.

[29] Ma T, Yang H, Lu L, Peng J. Pumped storage-based standalone photovoltaic power generation system: Modeling and techno-economic optimization, Applied Energy 2015; 137:649–659.

[30] Crettenand N. Small storage and pumped storage plants in Switzerland. Int Water Power Dam Construction 2012; 64 (4):22-24.

[31] Anagnostopoulos J.S, Papantonis D.E. Study of hybrid wind-hydro power plants operation and performance in the autonomous electricity system of Crete Island

[32] Bueno C, Carta J.A. Wind powered pumped hydro storage systems, a means of increasing the penetration of renewable energy in the Canary Islands. Renewable and Sustainable Energy Reviews 2006; 10(4):312-340.

[33] Kaldellis J.K, Kapsali M, Kondili E, Zafirakis D. Design of an integrated PV-based pumped hydro and battery storage system including desalination aspects for the Island of Tilos-Greece. In: Proceedings of International Conference on clean electrical power (ICCEP), Alghero, Sardinia, Italy, 2013.

[34] Melanie M. An Introduction to Genetic Algorithms. 5th ed. New. MIT Press Cambridge, Massachusetts; 1999.

[35] Malhotra R, Singh N, Singh Y. Genetic Algorithms: Concepts, Design for Optimization of Process Controllers, Computer and Information Science 2011; 4 (2): 39-54.

[36] Yang X.S. Firefly algorithm, stochastic test functions and design optimisation, International Journal of Bio-Inspired Computation 2010; 2: 78-84.

[37] Mirjalili S, Mirjalili S.M, Lewis A. Grey Wolf Optimizer, Advances in Engineering Software 2014; 69: 46-61.

[38] Sharma S, Mehta S, Chopra N. Grey wolf optimization for solving non-convex economic load dispatch, Engineering Research 2015; .3 (3): 17-21 .

[39] Wong, LI, Sulaiman, M.H. Mohamed, M.R. Hong, M.S . Grey Wolf Optimizer for solving economic dispatch problems. In: Proceedings of IEE conference on Power and Energy (PECon), 2014, pp 150-154.

[40] El-Gaafary, A.A.M, Mohamed Y.S, Hemeida A.M, Mohamed A.A. Grey Wolf Optimization for Multi Input Multi Output System, Communications and Network 2015; 3(1): 1-6.

[41] Yang H.X, Lu L, Burnett J. Weather data and probability analysis of hybrid photovoltaic–wind power generation systems in Hong Kong. Renew Energy 2003; 28:1813–1824.